Available online at www.sciencedirect.com
ScienceDirect
Applied Thermal Engineering 28 (2008) 728–737
APPLIED THERMAL ENGINEERING
www.elsevier.com/locate/apthermeng

The effects of frost thickness on the heat transfer of finned tube heat exchanger subject to the combined influence of fan types

Jeng-Min Huang [a,*], Wen-Chien Hsieh [a], Xin-Ji Ke [a], Chi-Chuan Wang [b]

[a] Department of Refrigeration, Air Conditioning National Chin-Yi University of Technology, Taichung County, Taiping City 411, Taiwan
[b] Energy and Environment Research Laboratories, Industrial Technology Research Institute, Hsinchu 310, Taiwan

Received 27 February 2007; accepted 8 June 2007
Available online 28 June 2007

Abstract

This study conducts a numerical study concerning the effect of frost thickness on the heat transfer performance of a four rows plate finned tube heat exchanger. Calculations are made under constant air volume and variable air volume conditions. It is found that the initial surge of heat transfer rate in the frosted finned tube heat exchanger is mainly associated with the critical radius effect rather than the surface roughness. The frost thermal conductivity plays an important role in the surge phenomenon. There is hardly any initial surge when frost thermal conductivity is below 0.1 W m^{-1} K^{-1}. It is also recommended that a refrigerator should defrost when half of a single flow channel area is blocked by frost. The calculations also reveal that a centrifugal fan is recommended with a small fin-pitch heat exchanger. However, if a long term operation at a thick frost situation is unavoidable, an axial fan should be selected. There is no great difference between selection of an axial fan or centrifugal fan for a larger fin pitch heat exchanger.

Keywords: Plate finned tube heat exchanger; Frost thickness; Fan

1. Introduction

The heat exchangers are widely used in various industrial equipments including HVAC, automobile, electronic equipments, and the like. The purposes of heat exchangers include heating, cooling, or heat recovery. The performance of a heat exchanger affects the effectiveness of the heat exchange and makes the study of heat exchanger becomes important in the energy saving research. For air-cooled heat exchangers used in the refrigeration or heat pump system, frost forms in the surface provided that the surface temperature is below the freezing point. The frost layer in the surface will increase the thermal resistance and the air pressure drops across the heat exchanger to degrade the overall performance. As a consequence, the investigation of frost properties and the effect of frost on the heat exchanger are important to improve the system performance. Yan et al. [1] experimentally investigated the performance of frosted finned tube heat exchangers of different fin types. The effects of the air flow rate, inlet air relative humidity, the refrigerant temperature, and the fin type on the thermofluid characteristics of the heat exchangers were discussed. Yang and Lee [2] proposed a mathematical model to predict the frost properties and relevant heat and mass transfer within the frost layer formed on a cold plate. Laminar flow equations for moist air and empirical correlations for local frost properties were employed to predict the frost layer growth. Yang and Lee [3] proposed dimensionless correlations for predicting the properties of frost formed on a cold plate. The air temperature, air velocity, absolute humidity, cooling plate temperature and frosting time were used to predict the properties of the frost layer. Lee et al. [4] presented a mathematical model to predict the frost layer growth and the characteristics of its heat and mass transfer by coupling the airflow with the frost layer. It is found that the heat transfer rate decreases rapidly at the early stage of frosting,

* Corresponding author. Tel.: +886 4 23924505; fax: +886 4 23932758.
E-mail address: jmh@ncit.edu.tw (J.-M. Huang).

1359-4311/$ - see front matter © 2007 Elsevier Ltd. All rights reserved.
doi:10.1016/j.applthermaleng.2007.06.020

Nomenclature

C_p	specific heat, J kg^{-1} K^{-1}
D_c	tube collar radius, mm
D_f	thickness of fin, mm
D_{fr}	thickness of frost, mm
P	pressure, Pa
h	heat transfer coefficient, J m^{-2} K^{-1}
FP	fin pitch, mm
FS	fin space, mm
k_{fr}	frost thermal conductivity, W m^{-1} K^{-1}
P_t	transverse tube pitch, mm
P_l	longitudinal tube pitch, mm
Q	heat transfer rate for a channel between two fins, W
Q_T	total heat transfer rate of a heat exchanger of a prescribed size, W
V	velocity, m s^{-1}
X	length of domain in the x direction, mm
x, y	coordinate
ρ	density, kg m^{-3}

Subscripts

a	air
i	inlet
o	outlet
fr	frost
b	wall
f	fin

but the rate of decrement is reduced gradually with time. On the other hand, the latent heat transfer rate, contrary to the sensible heat transfer rate was maintained at an almost constant value. Sahin [5] developed a cylindrical frost column model for evaluation of the effective frost thermal conductivity during the crystal growth period. The effective frost thermal conductivity increased with time as a result of densification. Higher plate temperature results in a more dense frost layer with higher effective frost thermal conductivity. Iragorry et al. [6] reviewed and compared the available literature concerning frost properties, correlations, and mathematical models as well as the analytical tools. However, their work did not involve the frosted finned tube heat exchanger. Wang et al. [7] studied frost formation and the airside performance of a fin array by visual observation. They reported that the frost thickness at the fin base is thicker than that at the tip and increases with time but decreases with the frontal velocity. O'Neal and Tree [8] reviewed the available correlations in the literature about frost thickness, frost thermal conductivity, and heat transfer coefficient on frosting surfaces in simple geometries. They presented results at the laminar flow regions in internal flow associated with the frosting effect in the plate finned heat exchanger of the operating heat pump. Kondepudi and O'Neal [9] reviewed the available literatures on the effects of frost formation and growth on finned tube heat exchanger performance. Four important variables of heat exchanger performance were investigated: fin efficiency, overall heat transfer coefficient, pressure drop and surface roughness. Many researches showed that the initial surge of heat transfer coefficient is attributable to the increase of surface roughness. After the initial increase of heat transfer rate, the heat transfer rate is decreased gradually by adding thermal resistance from growing frost thickness. This argument is generally adopted to explain the increase of heat transfer rate of finned tube heat exchanger under frosting in the initial stage. In the recent frosting finned tube heat exchanger researches (Kondepudi and O'Neal [10], Yan et al. [11], Seker et al. [12], and Yang et al. [13]), the initial surge of heat transfer coefficient was also observed without any new explanations. Frost roughness was still the only reason for the initial increase of heat transfer rate of the finned tube heat exchanger. However, when we inspected the effect of surface roughness on heat transfer in the existing literatures, the surface roughness is only quite effective at the turbulent flow region (such as those shown in the Moody chart). Most HVAC finned tube heat exchangers are operated at the laminar region due to the narrow fin spacing. In this regard, it would be valuable to re-examine the cause of initial surge of heat transfer rate in the frosted finned tube heat exchanger. Mao et al. [14] and Yun et al. [15] studied the frost characteristics and heat transfer of air over a flat plate considering the frost roughness effect. Mao et al. [14] investigated the frost growth on a flat cold surface supplied by subfreezing turbulent, humid parallel air flow. The surface is classified into a smooth and rough frost region according to the range of plate surface temperature and air relative humidity. They correlated the heat and mass transfer coefficients for rough, smooth, and full data set separately. Yun et al. [15] modeled the heat and mass transfer coefficients using the modified Prandtl mixing-length scheme to examine the effects of frost roughness and turbulent boundary layer thickness. By taking into account the roughness effect in the model, the initial surge of heat transfer rate is seen in the predictive result, but is not found in the relevant experiments. Besides, if the surface roughness is the only reason for initial surge, it can be expected that the initial surge phenomenon should appear in both fin-tube and cold plate cases. However, no initial surge appeared in the experimental results of cold plates from Lee et al. [4] and Yun et al. [15]. Therefore, it is likely that the effect of surface roughness on initial surge may be less important. Except roughness, the initial surge

phenomenon should be caused by another more significant reason. It is well-known that surface roughness can increase the heat transfer rate in the turbulent flow regime, but whether the frost roughness effect is the main cause of initial surge of frosting finned tube heat exchanger remains to be verified. Yang et al. [16] built a model including both fin and tube heat transfer coefficients to predict the frosting behavior of variable fin-tube heat exchangers. The performance included the Nusselt number correlation with no surface roughness effect used in the model. The predicted and comparatively experimental results indicated the increase of heat transfer rate due to frost layer growth. Sommers and Jocobi [17] presented an analytic solution for frost coated fin-tube heat exchanger. The fin efficiency was calculated from a two-dimensional tube and a one-dimension radial fin model. Xia and Jacobi [18] expressed the exact solution of the fin efficiency and heat transfer of a fin-tube heat exchanger with the help of a numerical conduction solution. Xia and Jacobi [19] reviewed the data reduction methods for wet- and frosted-surface of the heat exchanger. The LMTD and LMED methods for data interpolation were also formulated. After comparing these two methods, UA-LMTD was found to be more accurate than that of HA-LMED.

During the frosting period of a finned tube heat exchanger, Niederer [20] reported that the decrease in the heat transfer coefficient and the corresponding air cooler capacity was directly related to the reduced airflow rate resulting from frost accumulation on the coil surfaces. The reduction of airflow rate during the frosting period depends on the type of fan used. Chen et al. [21] studied the frosted parallel plate heat exchanger with different fans. Their results showed that the selections for the fan, fin spacing, and fin thickness may alter the frost growth and cycle time between defrosts of the heat exchangers. Xia et al. [22] experimentally investigated the performance of heat exchangers during initial frosting, defrosting and refrosting processes. The overall heat transfer coefficient, pressure drop, j and f factors of the five folded–louvered-fin, microchannel heat exchangers were compared. As a foregoing discussion, one of the objectives of this study is to examine the influence of surface roughness on the initial surge. The second purpose of this study is to investigate the effects of the fan characteristics on the frosted heat exchanger. Both axial and centrifugal fans are examined in this study.

2. Physical model, governing equations and numerical method

In this study, simulations are made with four rows plate finned tube heat exchangers having staggered arrangements with four fin pitches (25.4, 12.7, 6.35, 4.23 mm). The geometries are shown in Fig. 1 and listed in Table 1. The computational domain include airflow channel, frost layer and aluminum fin. The following assumptions are made:

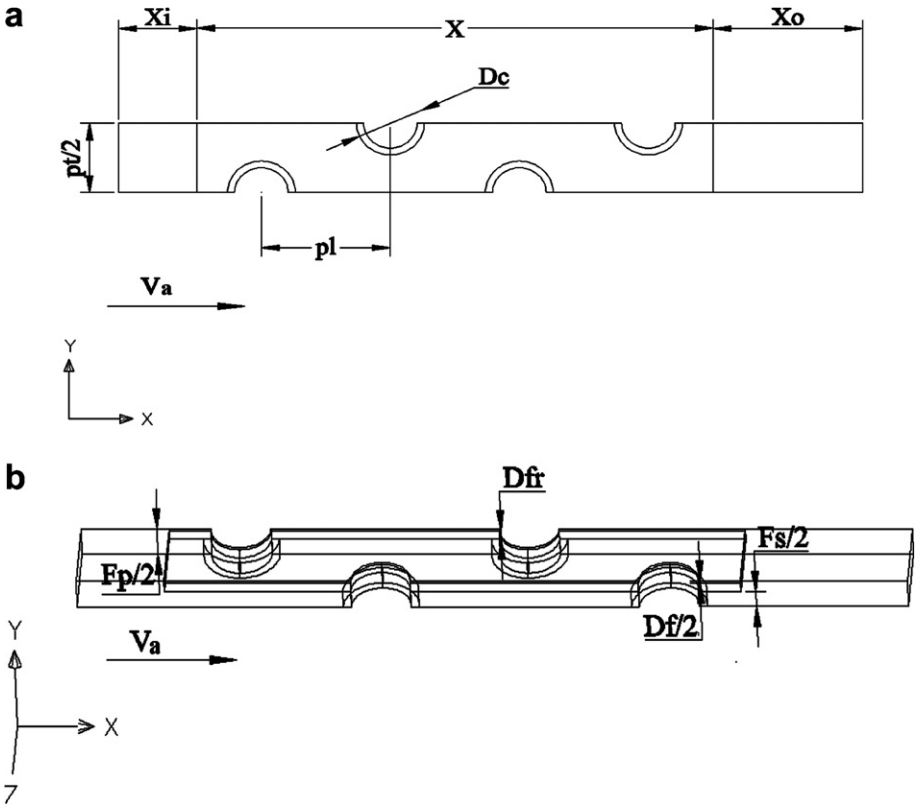

Fig. 1. The physical model of the frosted finned tube heat exchanger, (a) front view, (b) 3D view.

Table 1
Major dimensions of the heat exchanger

FP (mm)	25.4, 12.7, 6.35, 4.23	X_i	36.2 (mm)
P_t	21 (mm)	X	72.4 (mm)
P_l	18.1 (mm)	X_o	72.4 (mm)
D_f	0.25 (mm)	D_c	7.53 (mm)

1. Incompressible flow, constant properties, buoyancy force being neglected.
2. The frost layers that are formed on the fin and tube surfaces are homogeneous.
3. The heat transfer mechanism inside the frost layer is only via heat conduction and neglects the mass transfer.
4. According to the study of Mago and Sherif [23], the frost layer grows very slowly. Hence the quasi-steady process is assumed in the model. The variations of frost thickness, frost conductivity, and frost density during the frosting process are neglected.
5. Based on the studies of Ahmet [5] and Iragorry [6], two frost conductivities of 0.3 W m^{-1} K^{-1} and 0.1 W m^{-1} K^{-1} with frost density 300 kg m^{-3} are selected to cover the different frosting conditions. The ice specific heat 1930 J kg^{-1} K^{-1} is used in the computation.

The aluminum fin and air properties used in the computation are tabulated in Table 2. Boundary conditions of the computational domain are set as follows:

1. Uniform air velocity with a constant inlet temperature of 5 °C.
2. A free-gradient outlet boundary condition is set at the exit of the downstream extension.
3. The "symmetry" boundary is set at the two symmetrical planes.
4. No-slip boundary condition is set at all solid surface while the tube wall temperature is maintained at a constant temperature of −35 °C with conjugate heat transfer between the fin and frost layer.

Two kinds of generally used fans are used for the simulations, i.e., the axial and centrifugal fans. This can be made via including the fan characteristics represented by a pressure–air volume curve determined from several fan manufacturers and modified by the "fan law", in which the volume flow rate has been changed to a mean velocity. In Fig. 2, these two fans have a detectable difference in their performance curves and cause a different behavior after combination with a heat exchanger.

Table 2
Properties of the fin material and air

	Density (kg m^{-3})	Specific heat (J kg^{-1} k^{-1})	Thermal conductivity (W m^{-1} K^{-1})	Dynamic viscosity (kg m s)
Fin	2702	903	237	
Air	1.265	1006	0.02637	1.75×10^{-5}

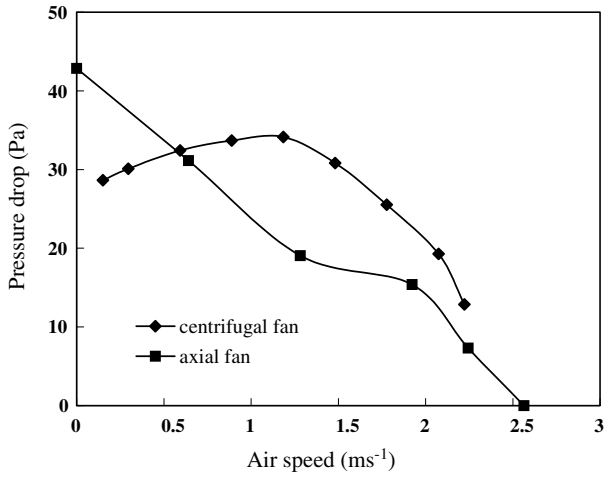

Fig. 2. Pressure–speed performance curve of axial and centrifugal fans.

A commercial CFD code Star-CD is used in this study to calculate the flow and temperature fields of frosted heat exchangers. Except for Leu et al. [24] using standard K–ε turbulent model, most previous researches like Jang et al. [25] and Mendez et al. [26] used laminar flow equations in the simulation of fin-and-tube heat exchanger. In this study, the wake flow at the exit of the heat exchanger might be in the transition or in turbulent flow region when the frost layer is thick enough. In that case, simulation may not converge by the laminar flow model. Therefore, low-Reynolds number K-ε model is applied in this study in order to calculate mixed flow fields (combined laminar, transition and turbulent flow types). A test of Low-Reynolds model is performed to examine the applicability of this model in the mixed flow field. Firstly, Low-Reynolds model is used to calculate a fully laminar flow field (a heat exchanger with 0.2 m s^{-1} inlet air velocity). The solution is almost the same as that of the calculation from the laminar equations. The eddy viscosities are very small compared with molecular viscosities. This indicates that the Low-Reynolds number turbulent model can be directly applied even at the laminar flow region. Then the inlet air velocity is increased to 2 m s^{-1}, calculated results of the flow field are shown in Fig. 3, where the eddy viscosities of the flow between fins are near zero, suggesting that a laminar flow region prevails. However, the eddy viscosity increases rapidly as the flow leaves the fins. In fact, the highest eddy viscosity in the wake is about 70 times higher than molecular viscosity (1.5×10^{-5} m^2 s^{-1}). Hence the flow is no longer laminar.

The following equations are used in this study:

Low Reynolds Number K–ε Turbulence model momentum equation (air side).
Low Reynolds Number K–ε Turbulence model energy equation (air side).
Heat conduction equation (fins and frost layer).

Detailed description of the turbulent model can be found in the Star-CD user's manuals. The mesh used in

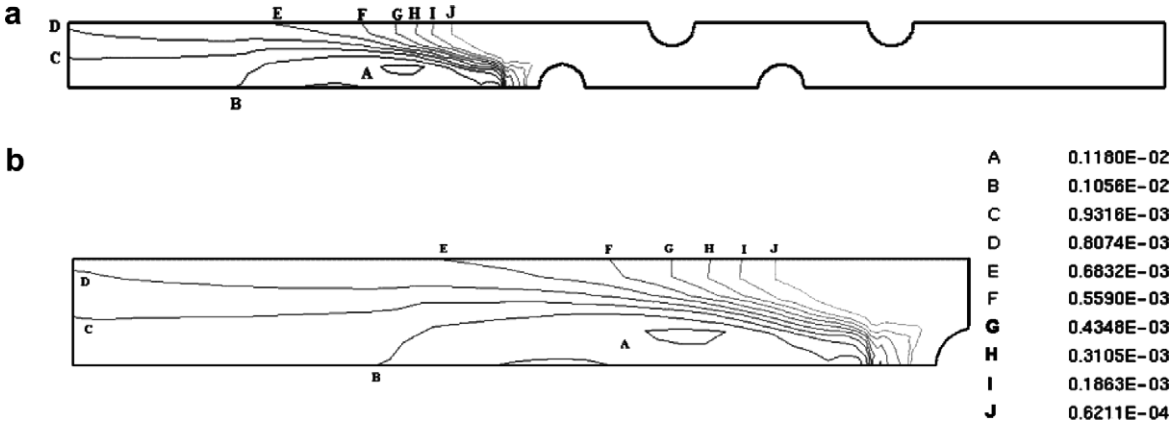

Fig. 3. The eddy viscosity distributions in the heat exchanger flow field (flow enters from right to left) (a) entire region, (b) wake zone.

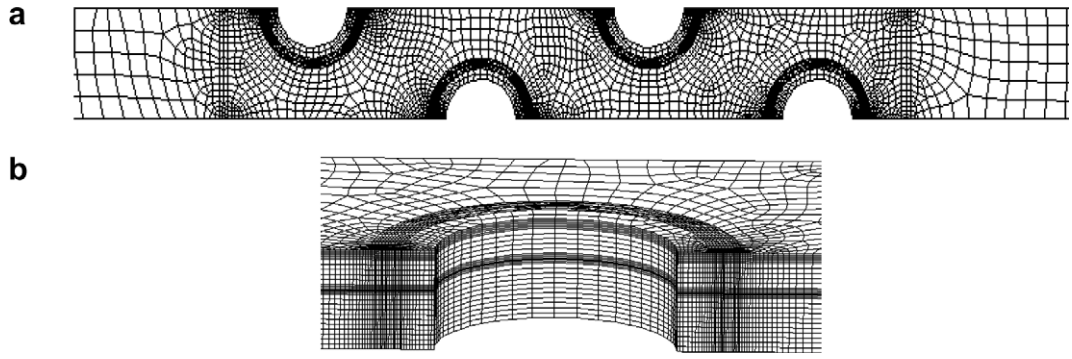

Fig. 4. Computational mesh used in the study, (a) x–y view, (b) near a pipe.

the study is shown in Fig. 4. Due to the complexity of the fin-tube geometry, an unstructured grid system is generated by "Auto Mesh" function of Star-CD for the airflow channel and the structured grid is used in the solid part. Star-CD is a finite-volume based CFD package. The central difference method is used to discretize the diffusion term and the convection term discretized by upwind difference method. SIMPLE scheme is applied on the iteration procedure. Numerical convergence is accepted only when the residuals of velocities, pressure, temperature and turbulent kinetic energy are smaller than 10^{-5}. Though the accuracy of the upwind method is not as good as other methods, the stability is the best of all. There are several flow separation regions in this study, especially a big wake in the outlet of the heat exchanger that makes the convergence of the numerical iterative process difficult. This is the reason why upwind method is used in this study and the accuracy could be improved by using more grids.

3. Results and discussion

A grid independence test is performed in the case of 2 m s^{-1} inlet air velocity, 6.35 mm fin pitch, 0.25 mm fin thickness and 1 mm frost thickness. Since the heat transfer rate affected by frost is regarded as the major variable, the heat transfer rate is selected as the grid independent test variable, and is compared with different meshes. Besides, energy unbalance between the tube side and the air side is also checked for different meshes. The energy unbalance of each mesh is required for a finite-volume based CFD code and should be carefully checked. This is because even the residual of the energy unbalance for each mesh is very small, their accumulation may grow to an unacceptable value. The grid independence test is shown in Table 3. It can be seen that the energy unbalance error for 151,890 meshes is 0.541% and the relative error between 151,890 and 213,350 meshes is 0.144%. To get a shorter computer time, sufficient accuracy, and an acceptable energy unbalance error, 150 thousand mesh numbers are used in all

Table 3
Results of numerical experiment of a single channel

	Number of mesh			
	61,206	122,956	151,890	213,350
Heat transfer rate (W)	1.13228	1.06278	1.06561	1.06715
Energy unbalance error	0.244%	0.415%	0.514%	0.407%
Relative error	6.957%	0.2656%		0.144%

cases in this study. From Table 3 it can be seen that the energy unbalance error of all meshes are below 10^{-5} with the total accumulated error up to 0.005.

In order to validate the accuracy of the simulation, calculations are compared with the experimental work from Wang et al. [27], and the comparisons are tabulated in Table 4. As seen in the table, the deviation between numerical and experimental results is about 12%, which is within the experimental uncertainty (3–15%). From the above validation, it is concluded that the simulation software is capable of solving the heat exchanger problem with reasonable accuracy.

The effect of frost thickness on heat transfer rate in a single channel with different fin pitches and frost conductivities under 2 m s^{-1} inlet air velocity is shown in Fig. 5. The frost layer has two effects on the heat transfer mechanism of the finned tube heat exchanger. The growth of frost thickness narrows the flow channel that leads to acceleration of the air velocity when the air volume is fixed, resulting in an increase of the air side heat transfer coefficient. Opposite to the heat transfer augmentation by flow contraction, the thermal resistance of the frost layer will be increased and will offset the conduction through the frost and fin. Hence, the effective total thermal resistance from air to the fin comprises of two parts: frost layer conductive thermal resistance and air flow convective thermal resistance, and is expressed as follows:

Conductive thermal resistance = frost thickness/(frost thermal conductivity × area).

Convective thermal resistance = 1/(heat transfer coefficient × area).

Therefore, the influence of frost growth on the heat transfer rate depends on the combined effects of increase of conductive resistance and decrease of convective resistance.

The effect of frost conductivity combined together with the influence of fin pitch is shown in Fig. 5. As seen in the figure, the heat transfer rate of fin pitch FP = 4.23 mm and 6.35 mm with $k_{fr} = 0.3$ W m^{-1} K^{-1} is increased with the growth of frost thickness mainly by accelerating the air velocity. However, one can see that when the frost conductivity is reduced to 0.1 W m^{-1} K^{-1}, the heat transfer rate declines monotonically with the frost thickness. Notice that the reduction of frost thermal conductivity not only increases the thermal resistance of the frost but also reduces the effective fin efficiency. In these two cases, the increment of heat transfer by flow acceleration may surpass the increased conductive thermal resistance caused by the frost layer. Unlike those of 6.35 mm and 4.23 mm fin pitch cases, the heat transfer rates of FP = 25.4 mm and 12.7 mm also decreased monotonically with frost thickness for both $k_{fr} = 0.3$ W m^{-1} K^{-1} and $k_{fr} = 0.1$ W m^{-1} K^{-1}. This is related to their larger fin spacing which diminishes the air acceleration effect on heat transfer caused by the frost layer. The decrease of heat transfer by the thermal resistance of the frost layer surpasses the increment of heat transfer by the flow acceleration, resulting in an overall decrease of the heat transfer rate.

Near the 0.1 mm frost thickness, the heat transfer rate of 25.4 and 12.7 mm fin pitches with $k_{fr} = 0.3$ W m^{-1} K^{-1} also reveals a slight overshoot. Kondepudi and O'Neal [9] argued that it is associated with the surface roughness in the early frosting stage. After checking the computational results, we have some different opinions to this phenomenon. Note that the heat transfer from air to heat exchanger can be divided into two parts, one is from the air across the frost to fin; the other one is direct across the frost to tube. Relevant heat transfer rates (through fin and direct to tube) of 0.1 mm frost thickness relative to an identical heat exchanger without frost are tabulated in Table 5 for detailed comparison. It is found that the heat transfer rate to the fin for the two cases (with and without frost) is nearly the same, but the heat transfer rate direct to the tube with a frost thickness of 0.1 mm is higher than that

Table 4
The comparison between results of the experiment [27] and computation

	Computational results	Experimental results [27]	Deviation
Heat transfer coefficient	47 W m^{-2} K^{-1}	42 W m^{-2} K^{-1}	11.9%

Heat exchanger dimensions: $P_t = 25.4$ mm, $P_l = 19.05$ mm, $D_c = 10.23$ mm, $V_{fr} = 1$ m s^{-1}.

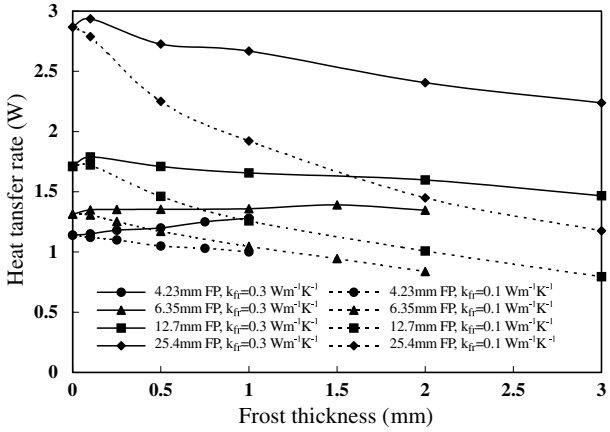

Fig. 5. The effect of frost thickness on the heat transfer rate for different fin pitches and frost thermal conductivities.

Table 5
Comparisons of heat transfer rate (W) to fin and direct to tube for a clear and 0.1 mm frosted surface

Fin pitch (mm)	No-frost fin (0 mm)	Clear tube (0 mm)	Fin (0.1 mm)	Tube (0.1 mm)
25.4	0.857	2.009	0.841	2.096
12.7	0.881	0.829	0.883	0.906

without frost. This is because the heat transfer rate to the fin is negligible with only 0.1 mm frost layer but on the contrary the heat transfer to the tube is increased about 10% by a critical radius effect ($=k_{fr}/h$). The average heat transfer coefficient in this case is about 73 W m^{-2} K^{-1} and the average critical radius of the tubes is about 4.1 mm which is appreciably larger than the tube radius (3.765 mm). There is no roughness effect taken into account in the computation. Based on the forgoing comments, the critical radius effect is suggested to be an important contribution to the initial surge. In the cases of 4.23 and 6.35 mm FP, the heat transfer rate directly to the tube is much smaller than that to the fin due to the larger fin to tube area ratio. As a result, the initial surge of heat transfer rate is not seen.

In a practical application, maintaining a constant air volume in an evaporator with a growing frost layer is not realistic, since the heat exchanger is usually operated with an axial or centrifugal fan. The corresponding flow resistance affects the flow rates considerably. Hence the pressure drops of flow resistance subject to different inlet air speeds, frost thicknesses and fin pitches are computed separately. A typical result is shown in Fig. 6 which represents the combination of fan curves (Fig. 3) with system pressure drops of a 4.23 mm FP heat exchanger under different frost thickness. The intersections of the system pressure drop with the fan curve denote the actual operation points that determine the actual air flow rate in a heat exchanger with different frost layer thickness. Opposite to the constant air volume, the air flow rate is decreased by the growing frost layer along the fan curve. When the air volume is highly reduced, the centrifugal fan may surge and the flow becomes unstable whereas the axial fan will increase the pressure head steadily but with a stall in the middle region which will decrease the air volume faster.

Fig. 7 shows the heat transfer rates at different frost thicknesses for a 4.23 mm FP heat exchanger operated with axial and centrifugal fans. The frost layer in the surface restricts the flow and increases the pressure drop which rides along the fan curve. The heat transfer rates of both $k_{fr} = 0.3$ W m^{-1} K^{-1} and 0.1 W m^{-1} K^{-1} decrease compared with the constant air volume cases in Fig. 5 where the flow acceleration effect increases the heat transfer for $k_{fr} = 0.3$ W m^{-1} K^{-1} and slows the decrease rate for $k_{fr} = 0.1$ W m^{-1} K^{-1}.

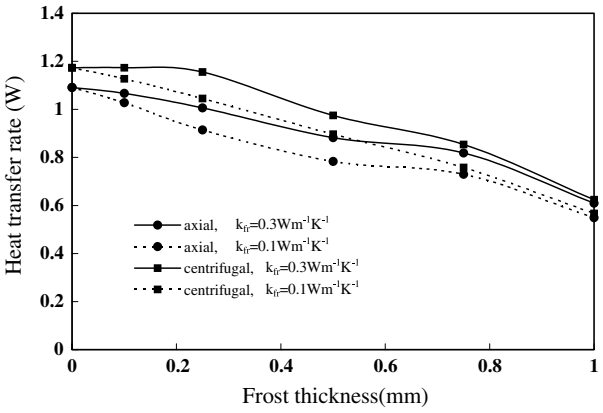

Fig. 7. The effects of frost thickness on heat transfer rate for a 4.23 mm FP heat exchanger operated with different type of fans.

In the stall region of an axial fan, the fan cannot manage the system flow resistance and the air volume may drop rapidly. This makes the heat transfer rate decrease faster when operated within this region (frost layer thickness between 0.1 mm and 0.5 mm). Because of the characteristics of the centrifugal fan, the heat transfer rate of the heat exchanger decreases faster than that with an axial fan when the frost layer begins to grow thicker (frost layer thickness between 0.5 mm and 1.0 mm).

The heat transfer rate of a 6.35 mm FP heat exchanger is shown in Fig. 8 which is quite similar to that of Fig. 7. But the initial surge (about 0.1 mm frost thickness) and the effect of fan type (from 1 to 2 mm frost thickness) are more pronounced in the result. The heat transfer rate for axial and centrifugal fans intersects during the frosting process. It is shown in Fig. 6 that the centrifugal fan could

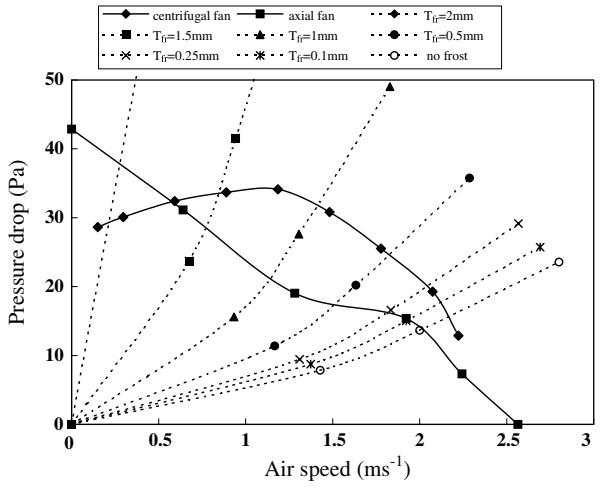

Fig. 6. Pressure drops combined with fan curves at different frost thickness for a 4.23 mm FP heat exchanger.

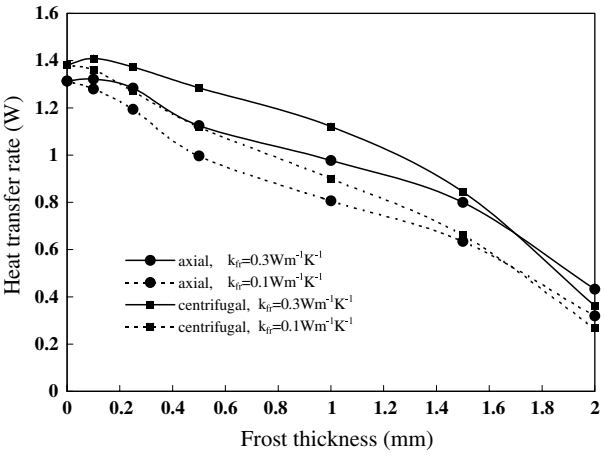

Fig. 8. The effects of frost thickness on heat transfer rate for a 6.35 mm FP heat exchanger operated with different type of fans.

withstand a low or medium flow resistance, but could not tolerate a high flow resistance because of the "surge" phenomenon appearing in the fan curve. By contrast, the axial fan can tolerate a much higher flow resistance. This would cause the air volume of heat exchanger operated with an axial fan to be higher than that of a centrifugal fan at thicker frost thickness. Thus, the heat transfer rate with an axial fan exceeds that with a centrifugal fan when the frost grows thicker.

Fig. 9 shows the heat transfer rates for a 12.7 mm FP heat exchanger operated with axial and centrifugal fans during frosting. The blockage ratio of flow channel with the same frost thickness is higher for a larger fin pitch heat exchanger relative to the one with a smaller fin pitch. The reduction of air volume due to frosting in a small fin pitch heat exchanger is not so significant. This eventually leads to a smaller heat transfer rate as the air volume decreases slowly as shown in Fig. 9. Besides, the difference of heat transfer rate for a 12.7 mm FP heat exchanger in association with different fans is smaller than that of 6.35 mm FP and 4.23 mm FP. This is especially profound at $k_{fr} = 0.1\ W\ m^{-1}\ K^{-1}$. The main performance difference between centrifugal and axial fans is the ability of flowrate adjustment against system resistance. The flow resistance in a 12.7 mm FP heat exchanger is smaller than that of 4.23 mm FP and 6.35 mm FP with the same frost thickness. However one should notice that the effect of fan type is negligible in a small fin pitch heat exchanger which leads to similar curves for axial and centrifugal fans. Fig. 10 shows the results of a 25.4 mm FP heat exchanger. Due to its considerable large fin spacing, the heat transfer rate of 25.4 mm FP heat exchanger decreases more slowly with the rise of the frost layer. A slight overshoot value of the heat transfer rate is also seen in $k_{fr} = 0.1\ W\ m^{-1}\ K^{-1}$. The influence of fan type on a 25.4 mm FP heat exchanger is still weaker than the other fin pitch.

The heat transfer rate shown in Figs. 7–10 is only applicable for one flow channel. To compare a heat exchanger

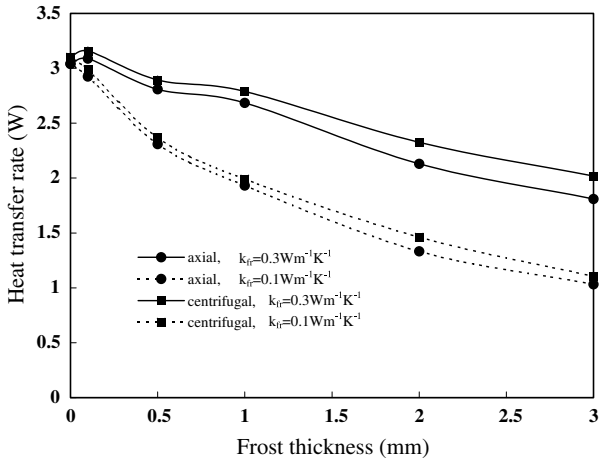

Fig. 10. The effects of frost thickness on heat transfer rate for a 25.4 mm FP heat exchanger operated with different type of fans.

of the same size with different fin pitches, four heat exchangers (25.4, 12.7, 6.35, 4.23 mm FP) with 0.3048 m (1 ft) in width are calculated and compared. The heat transfer rate operated with an axial fan is shown in Fig. 11. As expected, when frost thickness is smaller than 0.9 mm, the total heat transfer rate of 4.23 mm FP heat exchanger is the highest among the simulations for its largest surface area. However, the 6.35 mm FP heat exchanger shows the highest total heat transfer rate when the frost thickness is between 1 mm to 1.75 mm. When the frost thickness grows to 2 mm, about 2/3 channel width of the 6.35 mm FP heat exchanger is blocked and the flow resistance becomes so large so as to offset the heat transfer rate of a 6.35 mm FP heat exchanger, leading to a smaller heat transfer rate than that of a 12.7 mm FP heat exchanger.

The total heat transfer rate of a 25.4 mm FP heat exchanger is generally the lowest among the simulated samples for its smallest surface area. However, the difference decreases gradually as the frost layer thickness increases. The total heat transfer rate becomes the same as a

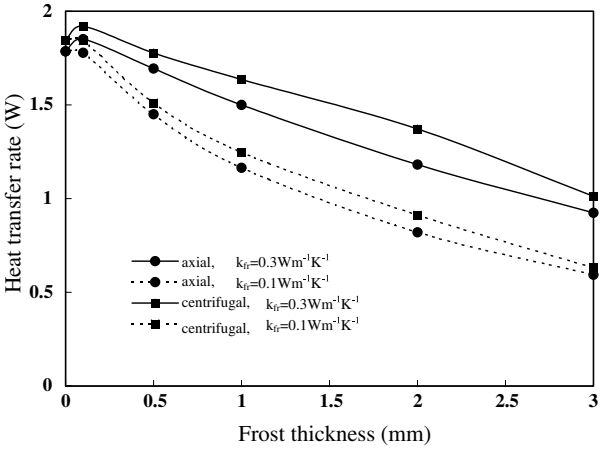

Fig. 9. The effects of frost thickness on heat transfer rate for a 12.7 mm FP heat exchanger operated with different type of fans.

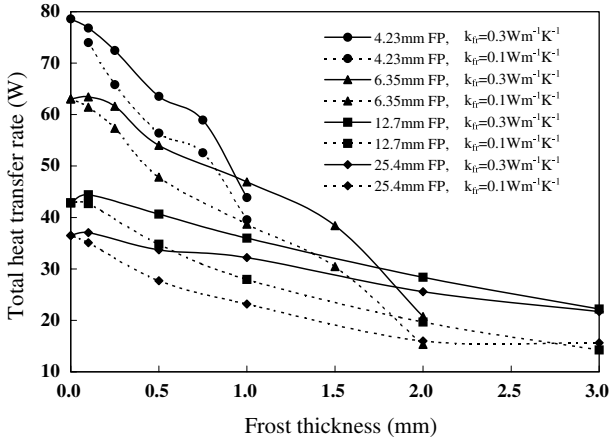

Fig. 11. The effects of frost thickness on total heat transfer rate of the same size heat exchanger for different fin-pitch, operated with axial fan.

12.7 mm FP heat exchanger when the frost layer thickness grows to 3 mm. Although the total heat transfer rate of 25.4 mm FP heat exchanger would exceed that of a 12.7 mm FP heat exchanger when the frost thickness is larger than 3 mm, it is only about half of that without frost. The total heat transfer rate for heat exchangers operated with centrifugal fan is shown in Fig. 12. By a careful examination of Figs. 12 and 11, it is found that the locus of 4.23 mm FP intersects with the 6.35 mm FP at a frost thickness of around 0.85–1 mm. Locus of the 6.35 mm FP heat exchanger intersects that of a 12.7 mm FP heat exchanger at frost thickness of 1.65–1.75 mm. Locus of the 12.7 mm FP heat exchanger intersects that of 25.4 mm FP heat exchanger at a frost thickness of about 3 mm. The heat exchangers operated with different kinds of fans have similar intersection points between heat transfer rates of different fin pitch heat exchangers.

From the forgoing discussions we found that the heat exchanger with the smaller fin pitch is more beneficial at a thin frost condition (or no frost) since it has a larger surface area. However, the advantage of having a larger surface area diminishes when frost is accumulated further. This is associated with the blockage of air flow. For a 4.23 mm FP heat exchanger, it could be seen from Figs. 11 and 12 that the total heat transfer rate of a 4.23 mm FP heat exchanger is about the same as that of a 6.35 mm FP heat exchanger when the frost layer thickness is about 0.9 mm. In this situation, about half of the flow channel is blocked by frost and fin (frost thickness = 0.9 mm × 2, fin thickness = 0.25 mm, fin pitch = 4.23 mm). The total heat transfer rate of a 6.35 mm FP heat exchanger is about the same as a 12.7 mm heat exchanger at 1.65 mm frost thickness. In this condition, about half of the flow channel is blocked by frost and fin (frost thickness = 1.65 mm × 2, fin thickness = 0.25 mm, fin pitch = 6.35 mm). The total heat transfer rate of a 12.7 mm FP heat exchanger is about the same as a 25.4 mm FP heat exchanger at 3 mm frost thickness. Similar to the above two cases, approximately half of the flow channel is blocked by frost and fin (frost thickness = 3 mm × 2, fin thickness = 0.25 mm, fin pitch = 12.7 mm). Hence it is concluded that the total heat transfer rate of a heat exchanger is about the same relative to a heat exchanger with larger fin-pitch when half of the flow channel is blocked. A further growth of frost thickness would substantially reduce the total heat transfer rate when compared to that of a larger fin pitch heat exchanger.

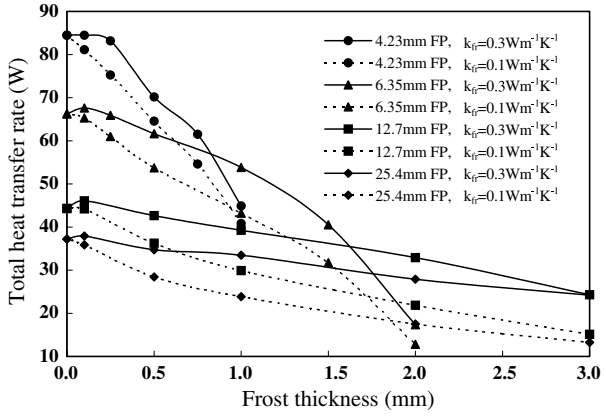

Fig. 12. The effects of frost thickness on total heat transfer rate of the same size heat exchanger for different fin-pitch, operated with centrifugal fan.

The purpose of defrosting is to maintain the performance of a refrigeration system. In practice, the frosted evaporator must be defrosted periodically. The defrost cycle will certainly affect the system performance and the product quality. An excessive defrost will increase the cooling load of a refrigerating equipment, resulting in a cyclic variation of the stored product temperature, even thawing and freezing the product repeatedly. In summary, how to select a proper evaporator and determine the defrosting cycle is an important issue in the design and operation of the refrigeration system. The present half-blockage fin pitch viewpoint provides an effective way to select a proper evaporator and its defrosting cycle. It is suggested that defrosting takes place for the frosted heat exchanger when half of the flow channel is blocked. One should replace a larger fin-pitch heat exchanger if excessive defrosting occurs. Furthermore, a centrifugal fan is recommended with a small fin-pitch heat exchanger. However, if a long term operation at a thick frost situation is unavoidable, an axial fan should be selected. There is no significant difference between selection of an axial fan or centrifugal fan for a larger fin pitch heat exchanger.

4. Conclusions and suggestion

This study performs a numerical study concerning the effect of frost thickness on the heat transfer performance of a four rows plate finned tube heat exchanger. Calculations are made under constant air volume and variable air volume conditions. Based on the foregoing discussions, the following conclusions are made:

1. The initial surge of heat transfer rate in the frosted finned tube heat exchanger is related to the frost thermal conductivity. There is almost no surge phenomenon when the frost thermal conductivity is below 0.1 W m^{-1} K^{-1}.
2. The surface roughness has only minor influence on initial surge. By careful examination of the present analysis, the authors suggest that the main cause of the initial surge is associated with the critical radius effect instead of surface roughness.
3. A refrigerator should defrost when half of a single flow channel area is blocked by frost. The heat transfer rate will decrease rapidly if the frost grows continuously. It is suggested that the heat exchanger should be replaced by a larger fin-pitch heat exchanger if excessive defrosting takes place.

4. A centrifugal fan is recommended with a small fin-pitch heat exchanger. However, if a long term operation accompanied with a thick frost situation is inevitable, an axial fan should be selected. There is no great difference between selection of an axial fan or centrifugal fan for a larger fin pitch heat exchanger.

Acknowledgements

The last author acknowledges part of the Energy R&D foundation funding from the Bureau of Energy of the Ministry of Economic Affairs, Taiwan.

References

[1] W.M. Yan, Y.L. Hung, Y.L. Tsay, Thermofluid characteristics of frosted finned-tube heat exchangers, Int. J. Heat Mass Transfer 48 (2005) 3073–3080.
[2] D.K. Yang, K.S. Lee, Modeling of frosting behavior on a cold plate, Int. J. Refrig. 28 (2005) 396–402.
[3] D.K. Yang, K.S. Lee, Dimensionless correlations of frost properties on a cold plate, Int. J. Refrig. 27 (2004) 89–96.
[4] K.S. Lee, J.S. Lee, D.K. Yang, Prediction of the frost formation on a cold flat surface, Int. J. Heat Mass Transfer 46 (2003) 3789–3796.
[5] Z.S. Ahmet, Effective thermal conductivity of frost during the crystal growth period, Int. J. Heat Mass Transfer 43 (2000) 539–553.
[6] J. Iragorry, Y.X. Tao, S. Jia, A critical review of properties and models for frost formation analysis, HVAC&R Res. 10 (2004) 393–420.
[7] C.C. Wang, Y.J. Chang, S.J. Fan, W.J. Sheu, Some observations of the frost formation in fin arrays, Heat Transfer Eng. 25 (8) (2004) 35–47.
[8] D.L. O'Neal, D.R. Tree, A review of frost formation in simple geometries, ASHRAE Trans. 91 (2A) (1985) 267–281.
[9] S.N. Kondepudi, D.L. O'Neal, The effect of frost growth on extended surface heat exchanger performance: a review, ASHRAE Trans. 93 (2) (1987) 258–277.
[10] S.N. Kondepudi, D.L. O'Neal, The effects of different fin configurations on the performance of finned-tube heat exchangers under frosting conditions, ASHRAE Trans. 96 (2) (1990) 439–444.
[11] W.M. Yan, H.Y. Li, Y.J. Wu, J.Y. Lin, W.R. Chang, Performance of finned tube heat exchangers operating under frosting conditions, Int. J. Heat Mass Transfer 46 (2003) 871–877.
[12] D. Seker, H. Karatas, N. Egrican, Frost formation on fin- and- tube heat exchangers. Part II—Experimental investigation of frost formation on fin- and- tube heat exchangers, Int. J. Refrig. 27 (2004) 375–377.
[13] D.K. Yang, K.S. Lee, S. Song, Modeling for predicting frosting behavior of a fin–tube heat exchanger, Int. J. Heat Mass Transfer 49 (2006) 1472–1479.
[14] Y. Mao, R.W. Besant, H. Chen, Frost characteristics and heat transfer on a flat plate under freezer operating conditions: Part I, Experimentation and correlations, ASHRAE Trans. 105 (2) (1999) 231–251.
[15] R. Yun, Y. Kim, M. Min, Modeling of frost growth and frost properties with airflow over a flat plate, Int. J. Refrig. 25 (2002) 362–371.
[16] D.-K. Yang, K.-S. Lee, S. Song, Modeling for predicting frosting behavior of a fin–tube heat exchanger, Int. J. Heat Mass Transfer 49 (2006) 1472–1479.
[17] A.D. Sommers, A.M. Jacobi, An exact solution to steady heat conduction in a two-dimensional annulus on a one-dimension fin: application to frosted heat exchangers with round tube, J. Heat Transfer 128 (2006) 397–404.
[18] Y. Xia, A.M. Jacobi, An exact solution to steady heat conduction in a two-dimensional slab on a one-dimensional fin: application to frosted heat exchangers, Int. J. Heat Mass Transfer 47 (2004) 3317–3326.
[19] Y. Xia, A.M. Jacobi, Air-side data interpretation and performance analysis for heat exchangers with simultaneous heat and mass transfer: wet and frosted surfaces, Int. J. Heat Mass Transfer 48 (2005) 5089–5102.
[20] H. Niederer, Frosting and defrosting effects on coil heat transfer, ASHRAE Trans. 82 (1) (1976) 467–473.
[21] H. Chen, L. Thomas, R.W. Besant, Fan supplied heat exchanger fin performance under frosting condition, Int. J. Refrig. 26 (2003) 140–149.
[22] Y. Xia, Y. Zhong, P.S. Hrnjak, A.M. Jacobi, Frost, defrost, and refrost and its impact on the air-side thermal-hydraulic performance of louvered-fin, flat-tube heat exchangers, Int. J. Refrig. 29 (2006) 1066–1079.
[23] P.J. Mago, S.A. Sherif, Frost formation and heat transfer on a cold surface in ice fog, Int. J. Refrig. 28 (2005) 538–546.
[24] J.S. Leu, Y.H. Wu, J.Y. Jang, Heat transfer and fluid flow analysis in plate-fin and tube heat exchangers with a pair of block shape vortex generators, Int. J. Heat Mass Transfer 47 (2004) 4327–4338.
[25] J.Y. Jang, M.C. Wu, W.J. Chang, Numerical and experimental studies three-dimensional plate-fin and tube heat exchanger, Int. J. Heat Mass Transfer 39 (14) (1996) 3057–3066.
[26] R.R. Mendez, M. Sen, K.T. Yang, R.M. Clain, Effect of fin spacing on convection in a plate fin and tube heat exchanger, Int. J. Heat Mass Transfer 43 (2000) 39–51.
[27] C.C. Wang, K.U. Chi, C.J. Chang, Heat transfer and friction characteristics of plain fin-and-tube heat exchangers: Part 1: new experimental data, Int. J. Heat Mass Transfer 43 (2000) 2681–2691.